

Do Kyu Kim<sup>1</sup>, Seung Joon Baik<sup>2</sup>, Jeong Ik Lee<sup>1\*</sup>,

<sup>1</sup>Dept. of Nuclear & Quantum Engineering, KAIST, 373-1, Guseong-dong, Yuseong-gu, Daejeon, 305-701, Republic of Korea

<sup>2</sup>KAERI, 111, Daedeok-daero 989beon-gil, Yuseong-gu, Daejeon, Republic of Korea

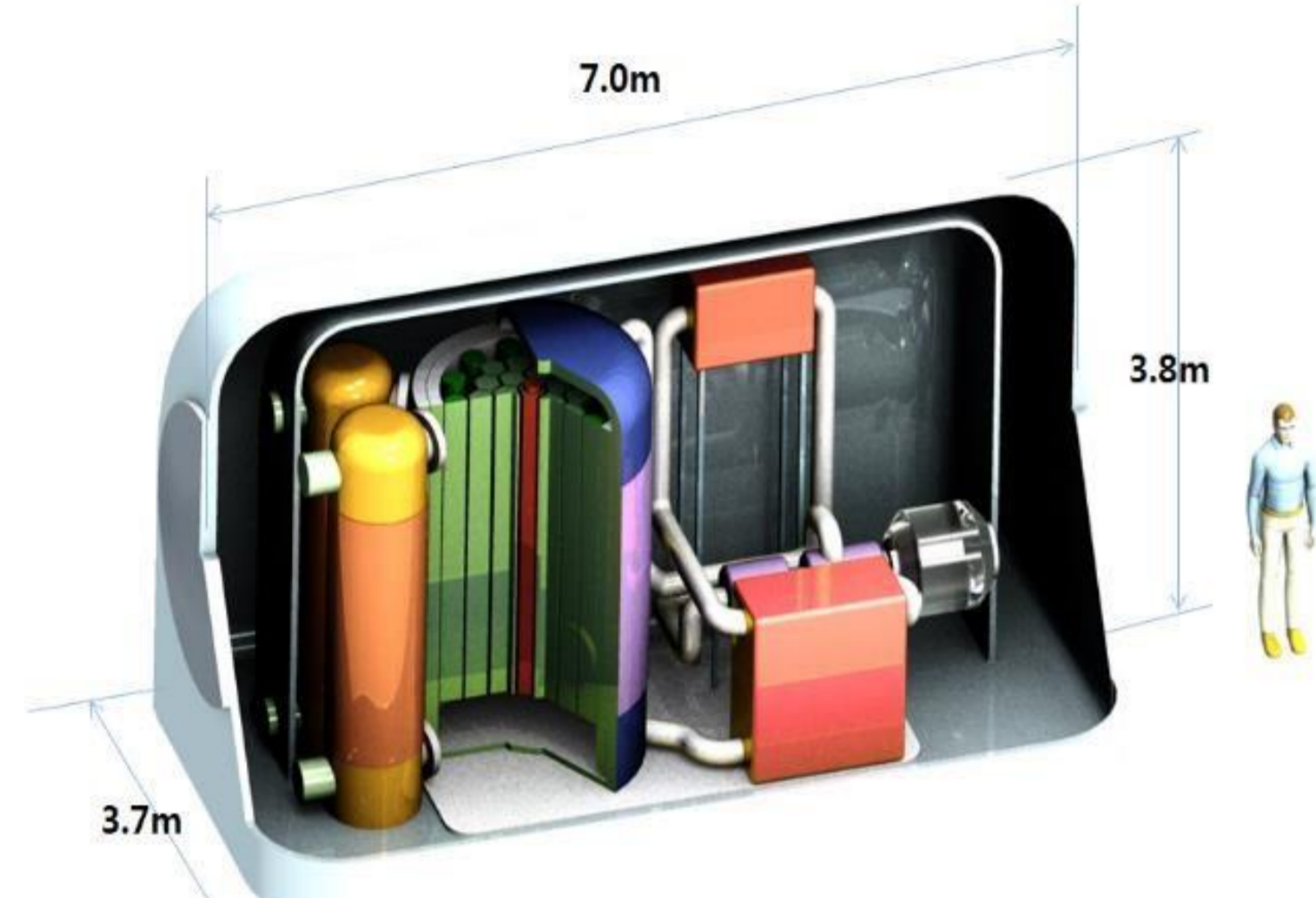
## Introduction & Background

### KAIST-MMR (MMR, Micro modular Reactor) 's Advantages

- MMR (fully modularized fast reactor with super critical CO<sub>2</sub>) has high power density with moderate heat source temperature.
- MMR can replace the diesel engine to avoid violating the newly released IMO regulation.

### Appropriate bearing selection

From the power scale of the MMR, magnetic bearing is well applicable. Oil lubricated bearing is excluded because oil supply and sealing system harms its compactness and independence.



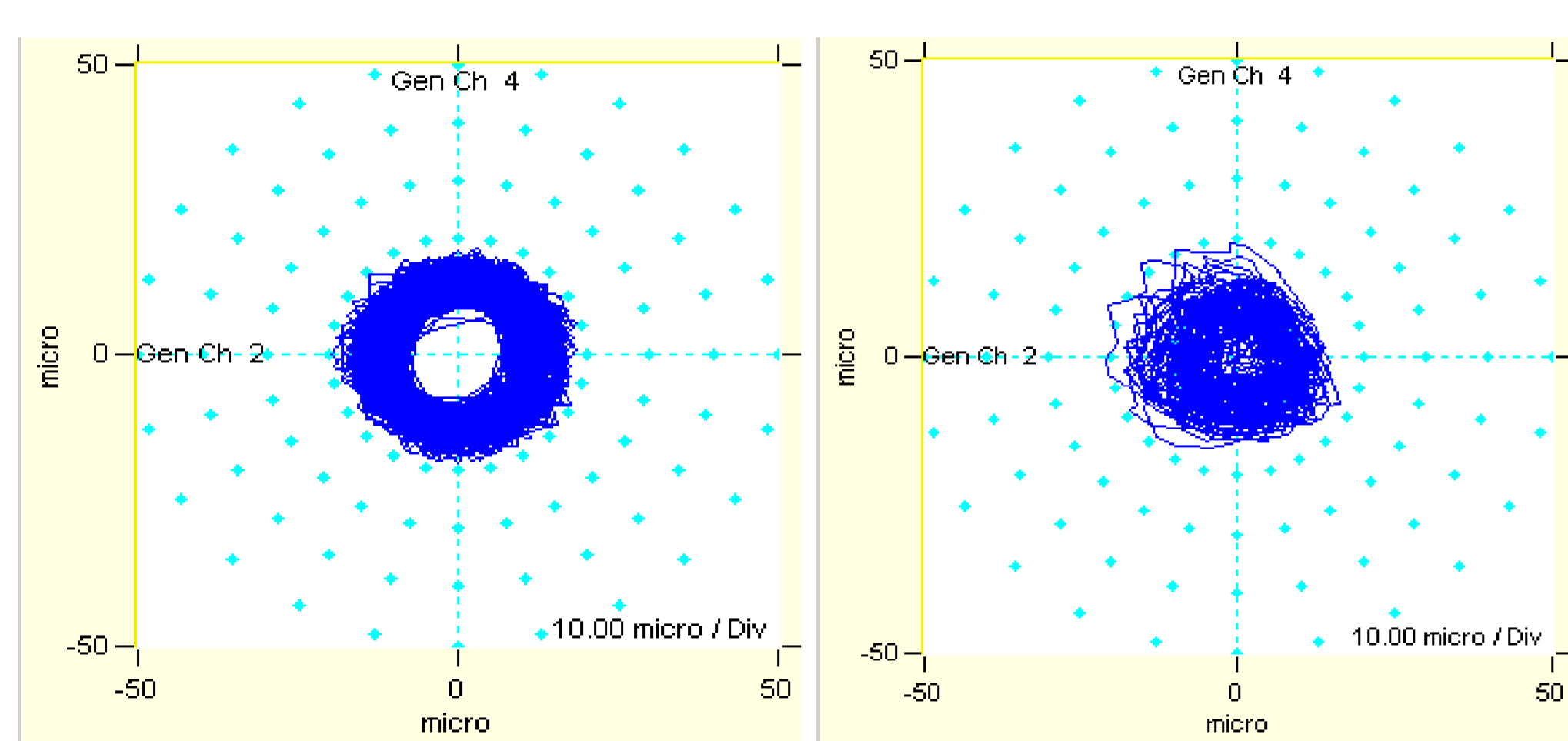
TM Feature	Power (MWe)					
	0.3	1.0	3.0	10	30	100
Bearings	Gas Foil			Hydrodynamic oil		
	Magnetic			Hydrostatic		

▲ Bearing options for S-CO<sub>2</sub> Brayton cycles with various power scales

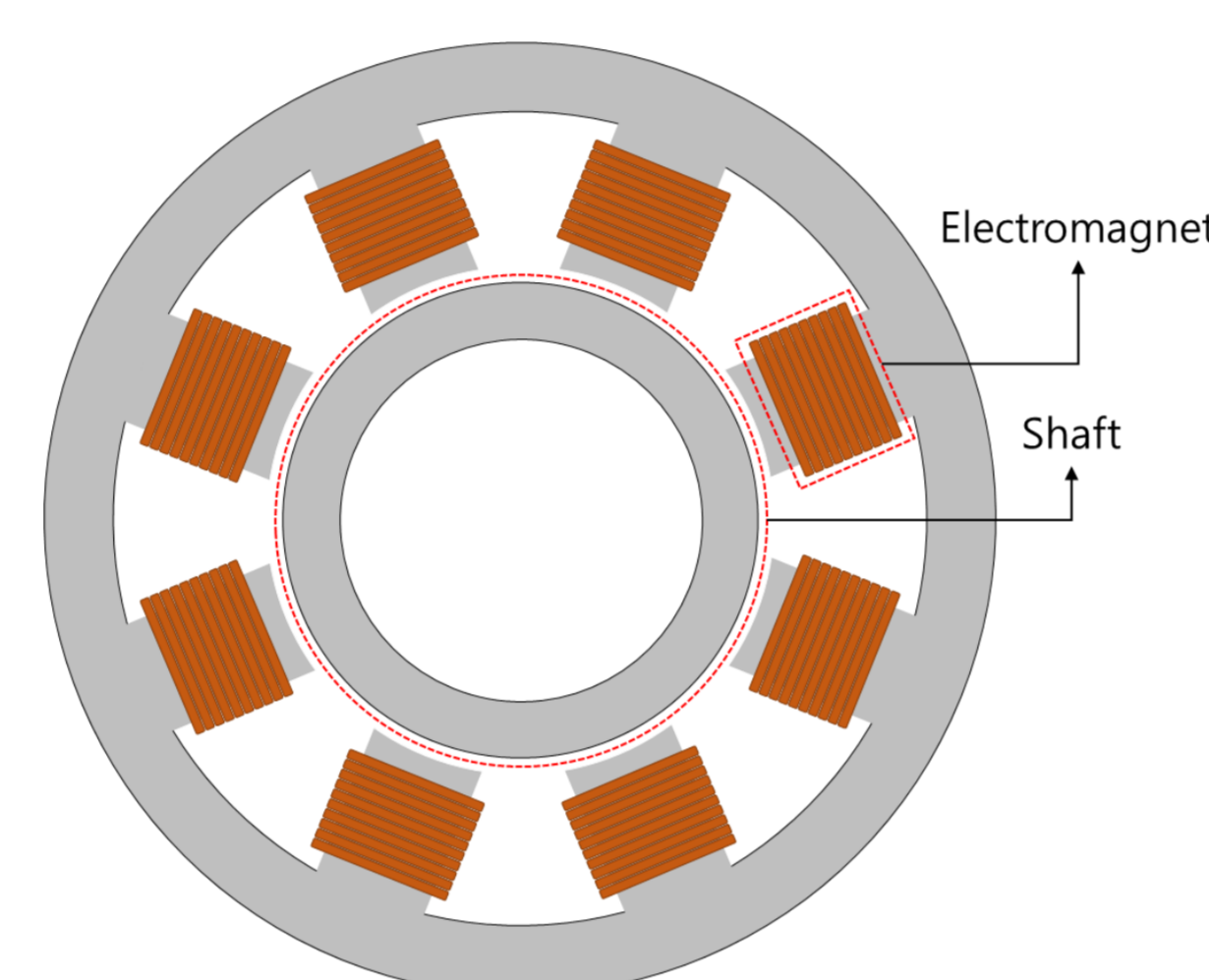
### Configuration of MMR

### Magnetic bearing's radial instability issue

- Under high pressure & high speed operation
- Shaft breakaways from the revolution orbit
- Leaked working fluid cools the rotor
- No such phenomenon with low density fluid



▲ Compressor shaft trajectory under air condition (left, 30000 RPM) and S-CO<sub>2</sub> condition (right, 14000 RPM)



▲ Cross-section of radial magnetic bearing

In this poster, the modeled S-CO<sub>2</sub> lubrication pressure distribution in the magnetic journal bearing geometry with uniform circular motion is analyzed with its physical properties. To explain and verify the results, the experimental results with shaft position is substituted into the model for comparison. Also, the results are analyzed with air gap's position.

## Modified fluid force analysis model

### Lubrication in magnetic bearing with inner coated geometry

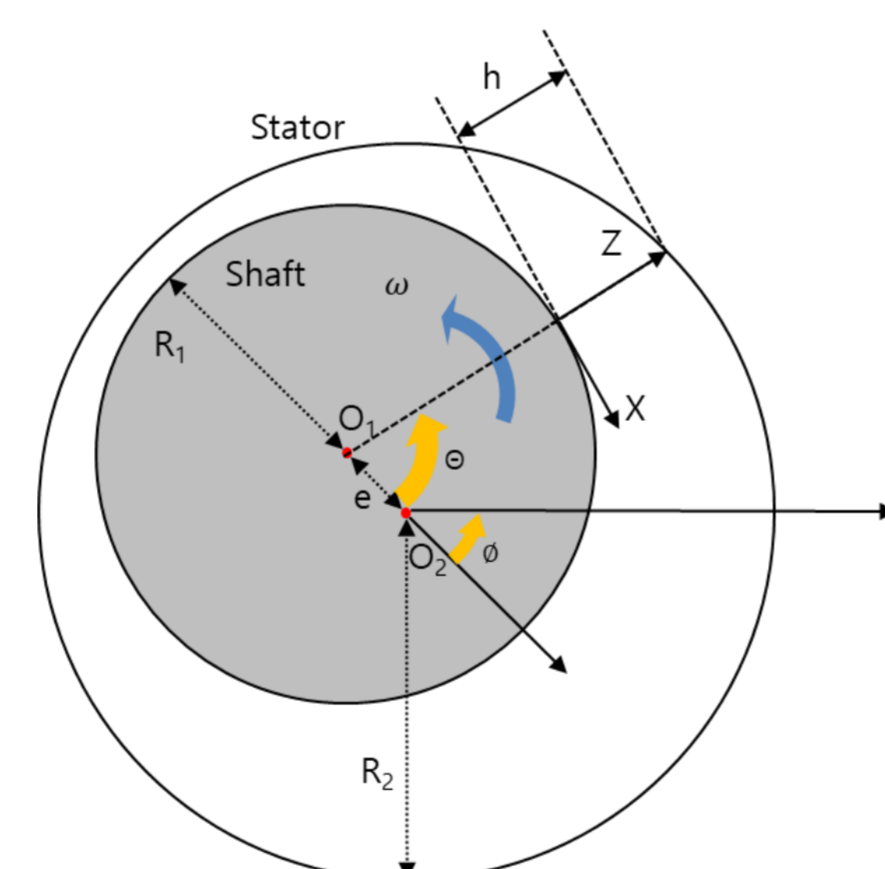
Magnetic bearing's electromagnet is exposed to the working fluid leaked through the labyrinth seal. Because the complex geometry is difficult to model, smooth geometry is analyzed with model at first.

### Fluid force model with Reynolds equation

- Thin film fluid dynamics equation
- Velocity profile from Navier & Stokes equation
- Substitute to the continuity equation
- Negligible axial direction & Quasi steady (perfect revolution)

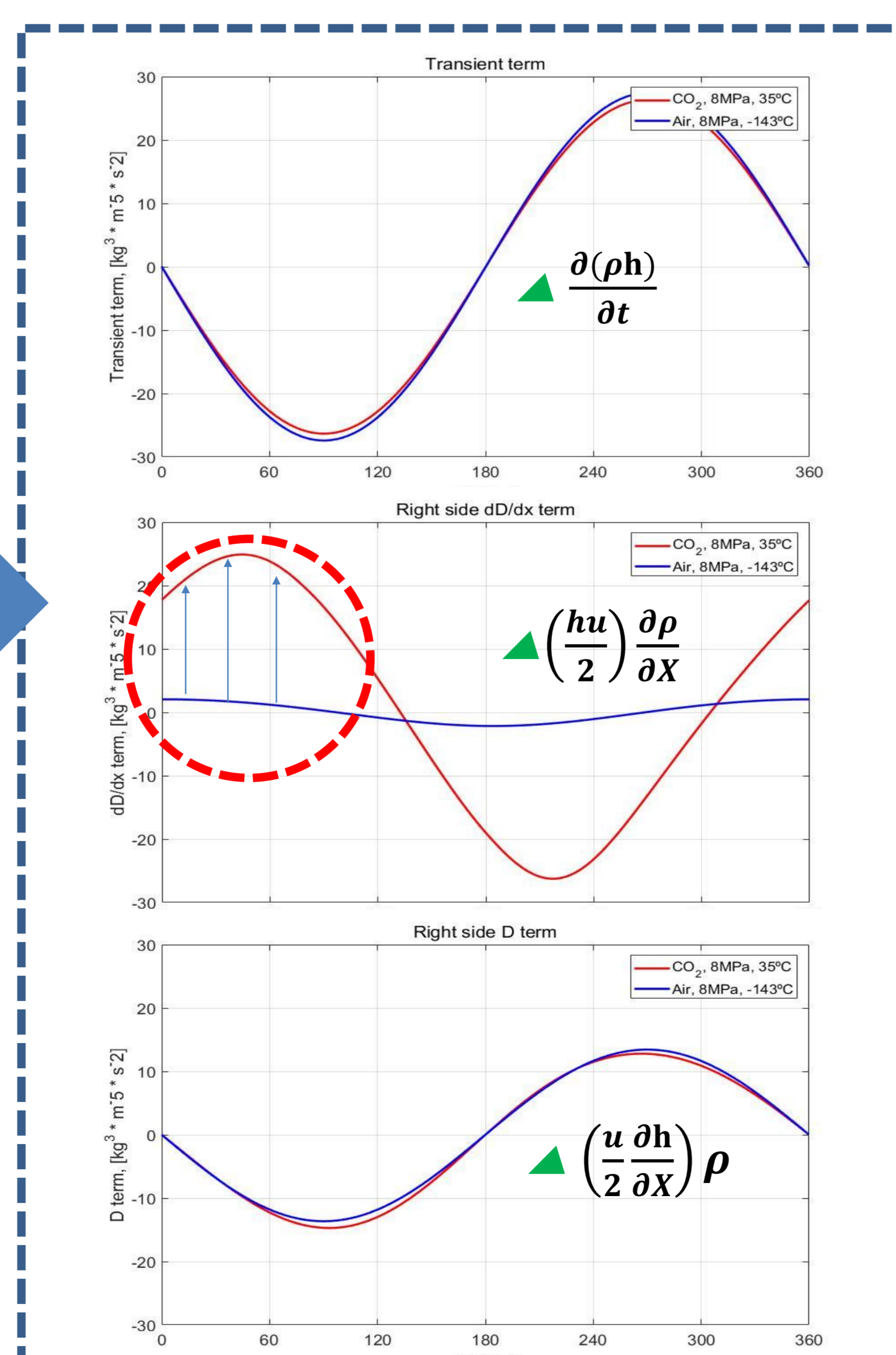
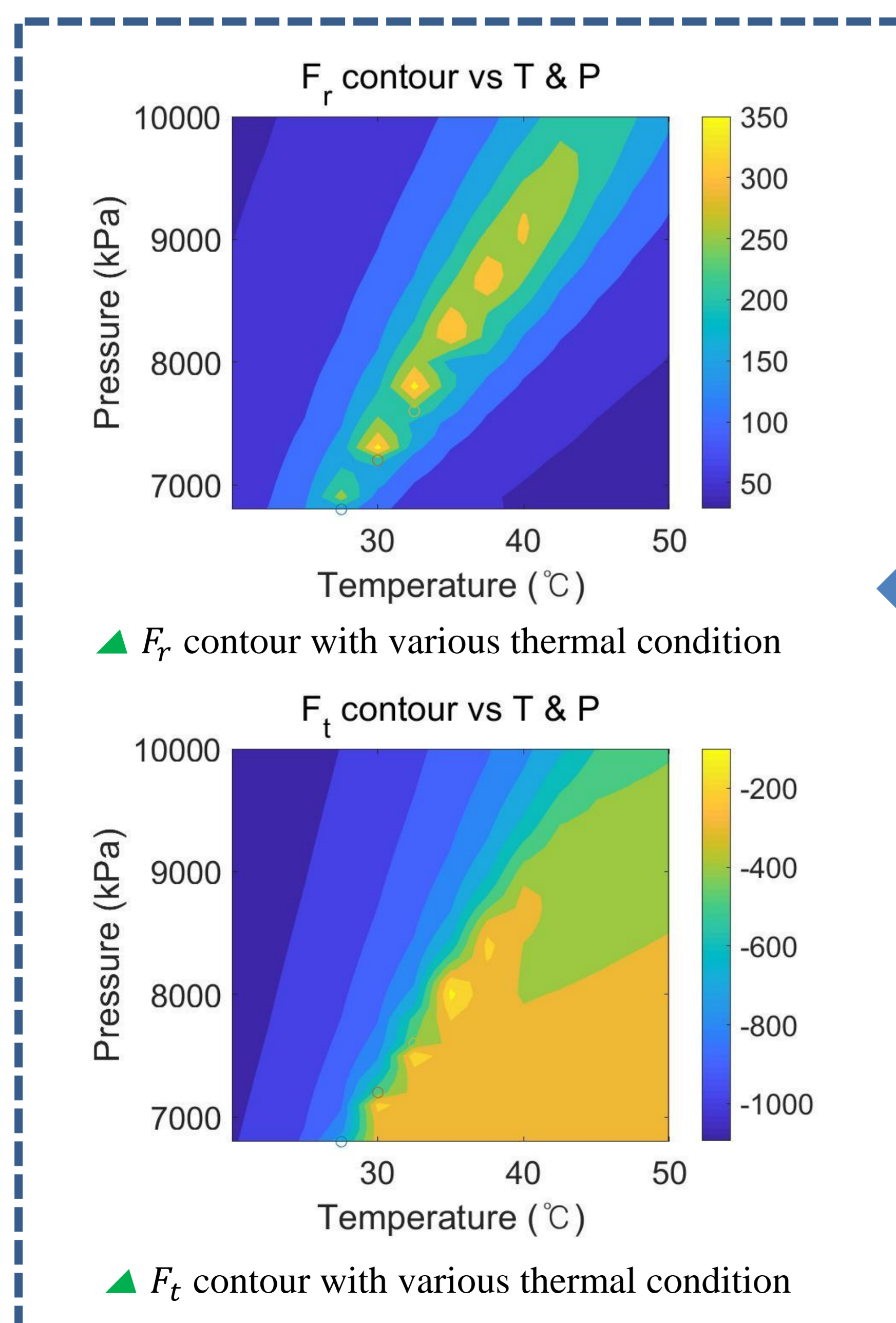
$$\frac{\partial}{\partial x} \left( \frac{\rho h^3}{12\mu} \frac{\partial p}{\partial x} \right) = \frac{\partial(\rho h)}{\partial t} + \frac{hu}{2} \frac{\partial \rho}{\partial x} + \frac{u}{2} \frac{\partial h}{\partial x} \rho$$

- Purpose : Pressure distribution & force exerted to the shaft



▲ Bearing modeling coordinate description

### Fluid force model results for 30,000 RPM and, ε (Eccentricity ratio)=0.08

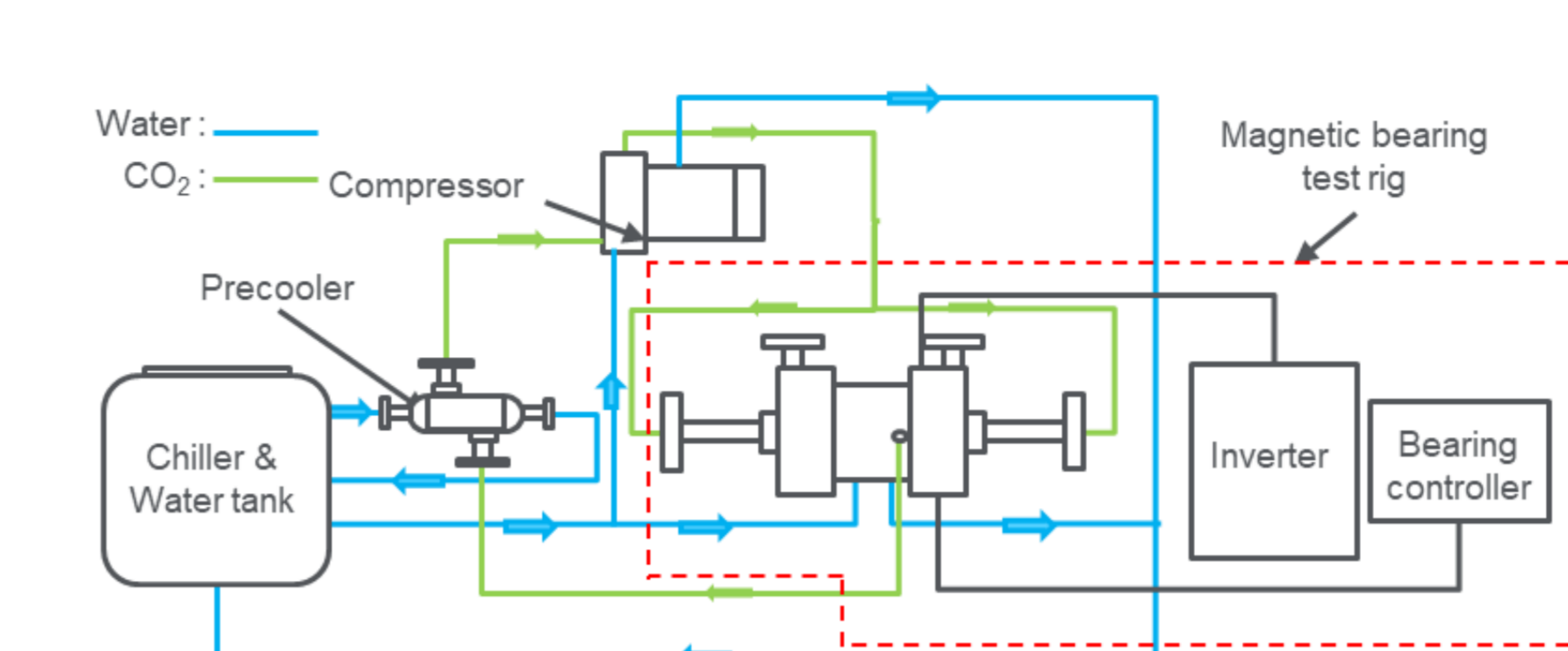


- High Density and its change is main reason of the fluid force gradient
- Control of thermal condition is required for experiment

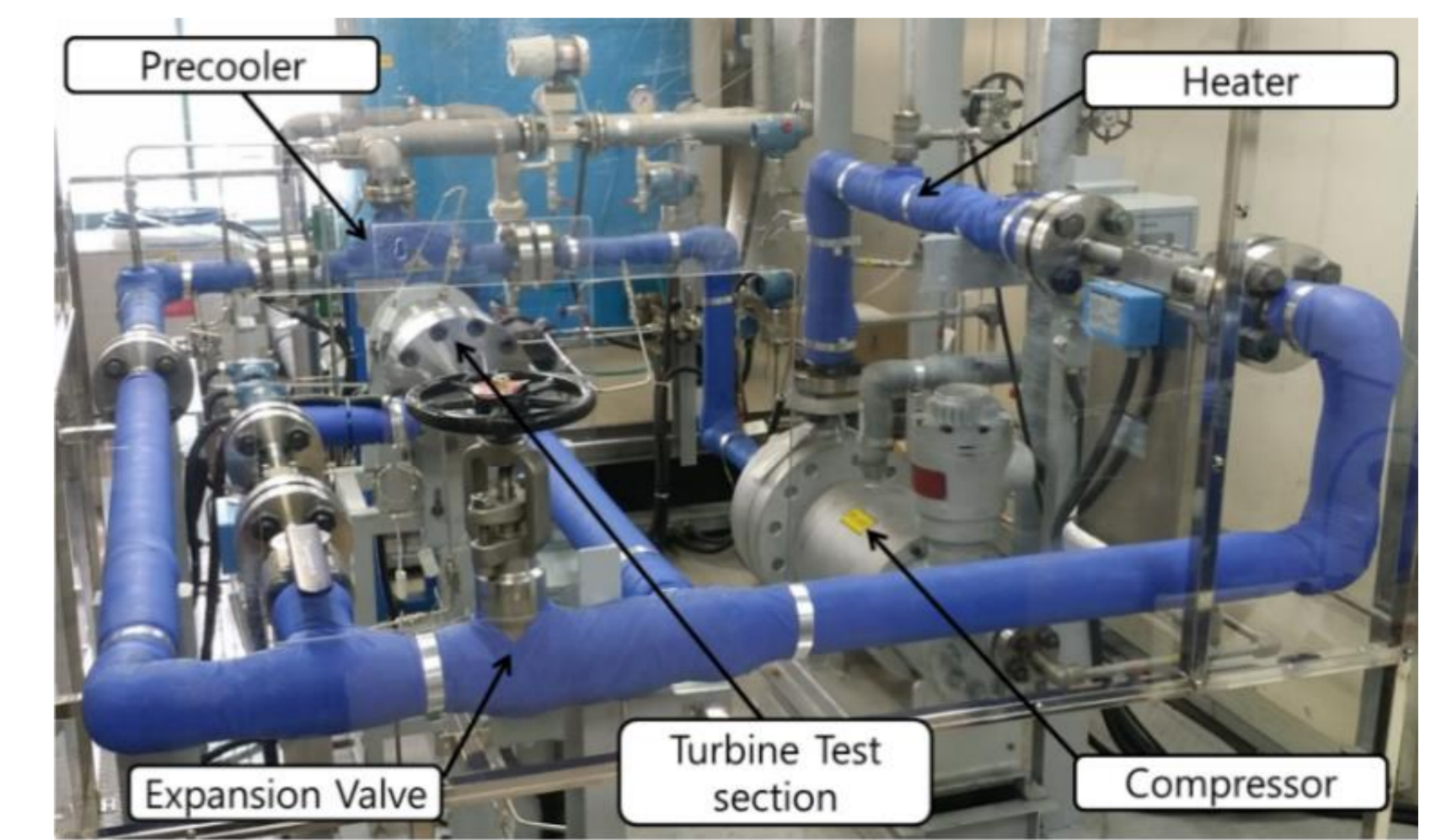
## Experimental study of magnetic bearing instability

### Layout of the experiment loop

The pump, chiller and heat exchanger are derived from the S-CO<sub>2</sub>PE which is S-CO<sub>2</sub> pressurizing loop constructed in KAIST to control the thermal condition



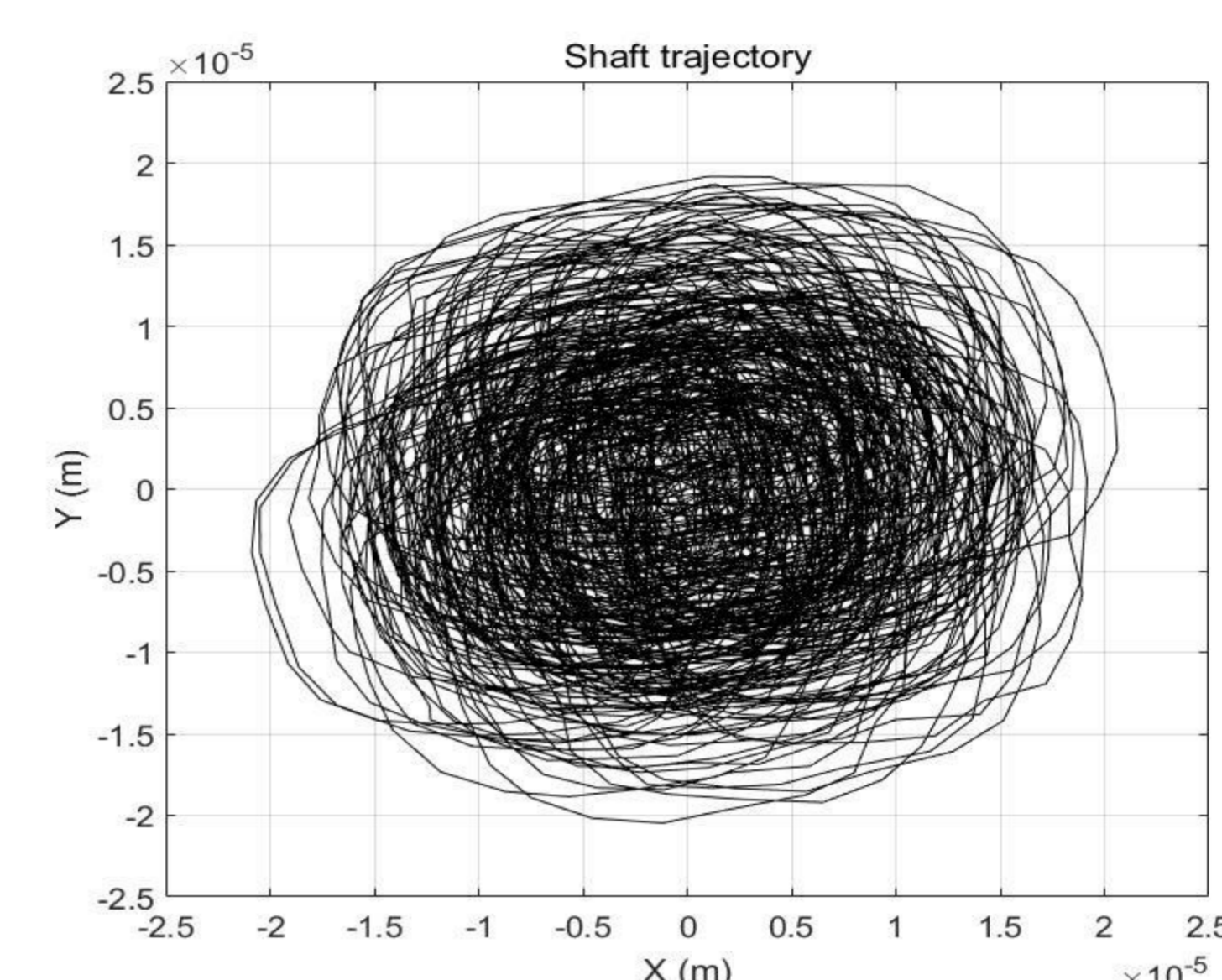
▲ Layout of the Bearing Instability Experiment



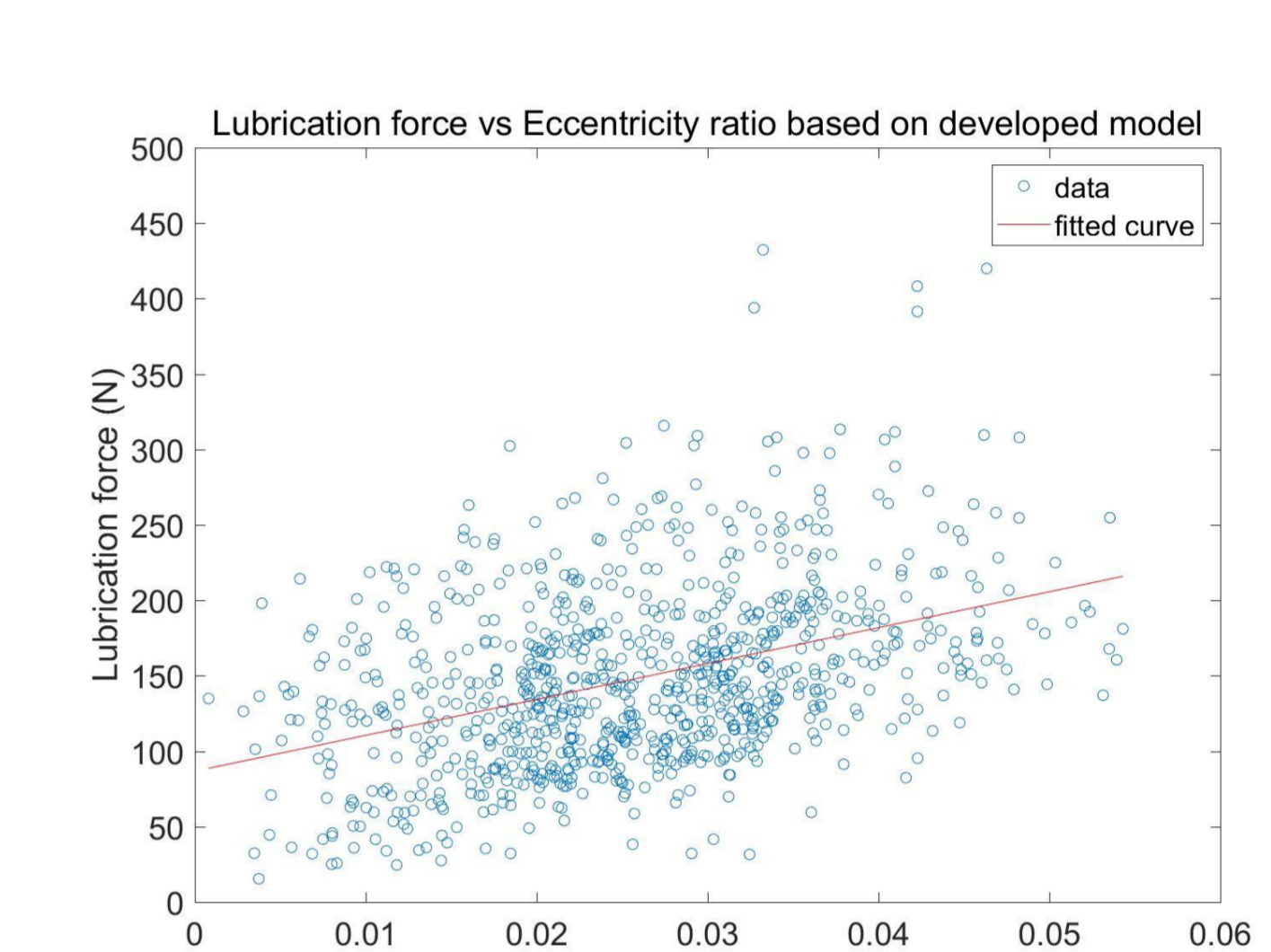
▲ S-CO<sub>2</sub> power cycle demonstration facility (S-CO<sub>2</sub>PE)

### Force analysis

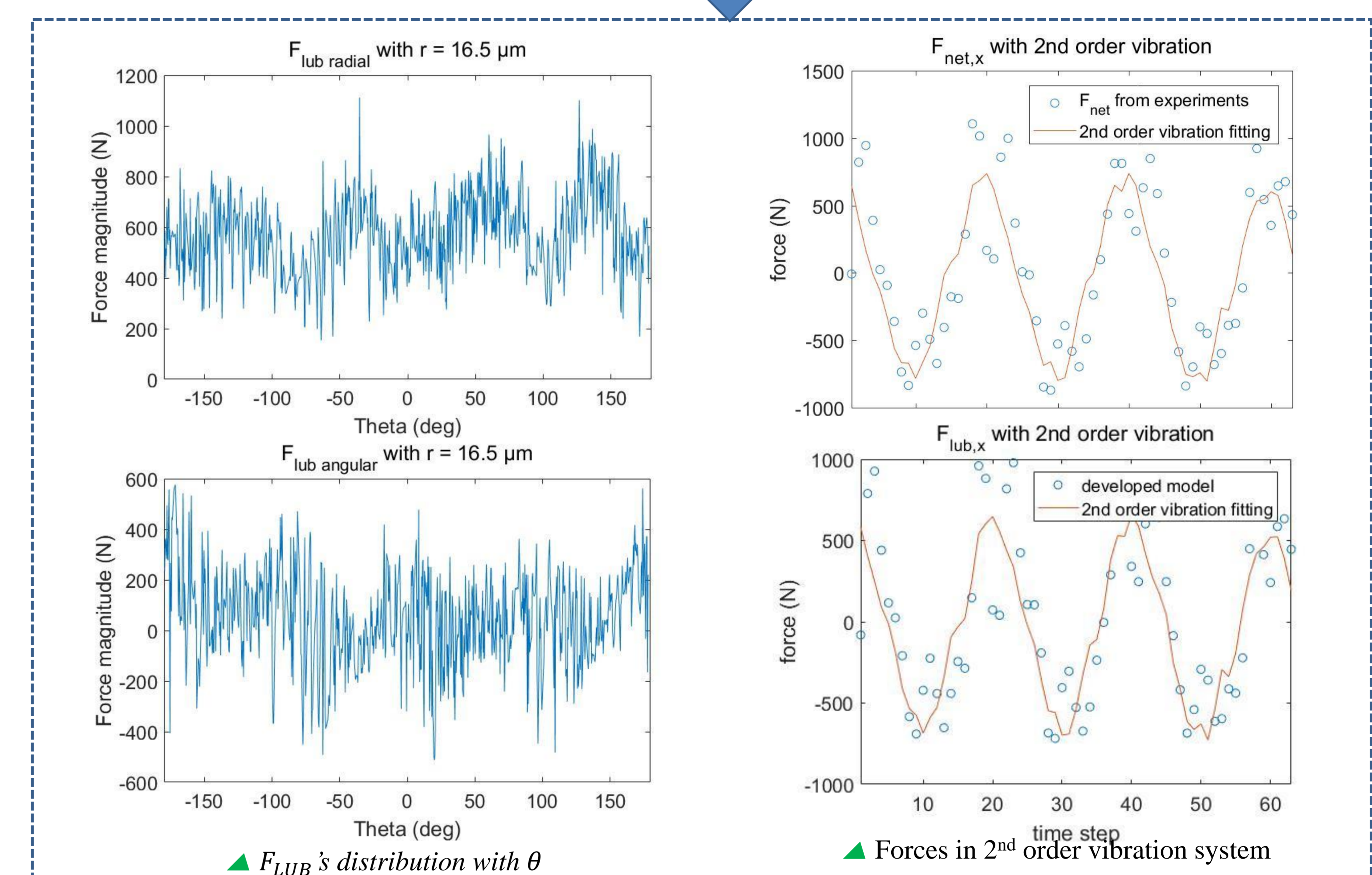
The shaft trajectory data is inserted to the developed fluid force analysis model. From this, the fluid force exerted on the shaft during the experiments are estimated. The calculated results are used to verify the model.



▲ Shaft trajectory with 8MPa, 36°C CO<sub>2</sub> and 30000 RPM condition



▲ F<sub>lub</sub> with 30,000 RPM



▲ F<sub>lub</sub>'s distribution with θ

▲ Forces in 2<sup>nd</sup> time step order vibration system

### Disturbance source

F<sub>lub</sub> has a period same as electromagnets array. The gaps between the electromagnets appear to cause the CO<sub>2</sub> flows that impede control.

### Vibration system analysis

F<sub>lub</sub> and F<sub>net</sub> follow the trend of the 2<sup>nd</sup> order system.

## Conclusions & Future work

### Insatbility source

Magnetic bearing's air gaps between the electromagnets appear to be the instability source

High density of S-CO<sub>2</sub> can be the instability source of the magnetic bearing levitation

This analysis cannot define the effect of the rapid angle change near pseudo-critical line

### State Space Analysis

$$\dot{X} = AX + Bu, X = \begin{pmatrix} \dot{x} \\ \dot{y} \\ x \\ y \end{pmatrix}, A = \begin{pmatrix} -\frac{C_{xx}}{m} & -\frac{C_{xy}}{m} & -\frac{K_{xx}}{m} & -\frac{K_{xy}}{m} \\ -\frac{C_{yx}}{m} & -\frac{C_{yy}}{m} & -\frac{K_{yx}}{m} & -\frac{K_{yy}}{m} \\ 1 & 0 & 0 & 0 \\ 0 & 1 & 0 & 0 \end{pmatrix}$$

- With A's eigenvalue, the vibration system's convergence can be predicted.
- AMB's control strategy can be designed with desired eigenvalue.
- The effectiveness of it is planned to be tested with several control strategy

